Optimal transport in time-varying small-world networks

Qu Chen,[1,2] Jiang-Hai Qian,[3] Liang Zhu,[4] and Ding-Ding Han[1,2,*]

[1]*Shanghai Key Laboratory of Multidimensional Information Processing, East China Normal University, Shanghai 200241, China*
[2]*School of Information Science and Technology, East China Normal University, Shanghai 200241, China*
[3]*School of Mathematics and Physics, Shanghai University of Electric Power, Shanghai 200090, China*
[4]*Shanghai Institute of Applied Physics, Chinese Academy of Sciences, Shanghai 201800, China*

The time-order of interactions, which is regulated by some intrinsic activity, surely plays a crucial role regarding the transport efficiency of transportation systems. Here we study the optimal transport structure by measure of the length of time-respecting paths. Our network is built from a two-dimensional regular lattice, and long-range connections are allocated with probability $P_{ij} \sim r_{ij}^{-\alpha}$, where r_{ij} is the Manhattan distance. By assigning each shortcut an activity rate subjected to its geometric distance $\tau_{ij} \sim r_{ij}^{-C}$, long-range links become active intermittently, leading to the time-varying dynamics. We show that for $0 < C < 2$, the network behaves as a small world with an optimal structural exponent α_{opt} that slightly grows with C as $\alpha_{opt} \sim \log(C)$, while for $C \gg 2$ the $\alpha_{opt} \to \infty$. The unique restriction between C and α unveils an optimization principle in time-varying transportation networks. Empirical studies on British Airways and Austrian Airlines provide consistent evidence with our conclusion.

I. INTRODUCTION

Transport efficiency is one of the primary concerns in network design and optimization of transportation systems, such as the Internet and airport networks. In the past decade, those networks are often viewed as static geographic-based graphs where nodes are embedded in a d-dimensional lattice. By allocating long-range connections between two distant nodes i and j with the probability $P_{ij} \sim r_{ij}^{-\alpha}$, the network turns into a small world within a specific range [1–5]. Theoretical studies have shown that there is a trade-off between short- and long-range connections to best optimize transport paths and ongoing traffic dynamics [6–12]. But the optimal conditions are far from unified. As found on the unconstrained Kleinberg model, the network diameter is minimized at $\alpha_{opt} = 0$ [9,13,14]. Imposing the cost limitation on additional links, the optimal exponent enlarges to $\alpha_{opt} = d + 1$ [15,16], while it shifts to a smaller value by introducing degree heterogeneity [17]. All these efforts provide us a better understanding of the optimal spatial structure for general transport dynamics.

Apart from the geometric topology, transport efficiency is also determined by the dynamic pattern of link interactions. In airline networks, for example, flights are running on predesigned air routes to transport passengers [18–22]. The time-ordered flight schedule is at the basis of travel time, whose inefficient design will dissipate structural convenience. For a passenger arriving at airport j from airport i at time t_1, his travel to k can continue only if there is a flight from j to k at time $t_2 > t_1$. Hence the transport path not only relies on the underlying topology, but also on how the edge activation events are ordered in time, which is the key character of time-varying systems [23–27]. In such a context, the temporal shortest path length T_{ij} is defined as the fastest time it takes to reach the target j from the source i along the time-respecting path. Taking temporal dimensions into account, some fundamental properties such as network connectivity, damage resilience,

and epidemic threshold are strikingly different from those of static cases [26,28–30]. Consequently, the problem of how well the network is optimized might go beyond our traditional knowledge.

On the other hand, interaction dynamics is not completely random but driven by intrinsic activity [31–35]. In transport systems, the activity potential of each route, i.e., the flight intensity or bus departure frequency, is implicitly involved in running schedules, whose design significantly considers geographical distance for cost savings. We believe that it is the close interplay between geometric structure and interaction dynamics that determines the transport efficiency, which is neglected in previous attempts. In this paper, we introduce the temporal effect into the classical Kleinberg model to determine the optimal behavior of the temporal shortest path. The paper is organized as follows. In Sec. II we propose a temporal model by relating the activity potential of shortcuts to their geometric lengths. In Sec. III, we discuss in detail the optimal transport structure of time-varying systems. Our empirical analysis on British and Austrian Airlines in Sec. IV unveils the relationship between flight schedule and underlying air-route structure, which confirms our theoretical prediction. Finally, we make a conclusion in Sec. V.

II. MODEL DESCRIPTION

To characterize the long-term pattern of contacts, we first construct the underlying network G_0 based on the classical Kleinberg model [2,3]. N nodes are arranged in a two-dimensional regular lattice and each node is connected with its four nearest neighbors. Additionally, each node has q long-range connections. Node i is connected to a distant node j with probability

$$p(r_{ij}) = \frac{r_{ij}^{-\alpha}}{\sum_{j \neq i} r_{ij}^{-\alpha}}, \tag{1}$$

where $r_{ij} = |r_i - r_j|$ is the Manhattan distance between node i and j, and α is a control parameter that determines the

*ddhan@ee.ecnu.edu.cn

magnitude of both short- and long-range connections. The larger the parameter α, the shorter are the long-range shortcuts.

To our assumption, link dynamics over the underlay is driven by the internal activity potential. Each shortcut l_{ij} is characterized by an activity rate τ_{ij}, derived from its geometric length r_{ij} in the following form [36]:

$$\tau_{ij} \sim r_{ij}^{-C}, \tag{2}$$

where C is the coupling strength which determines to what extent the link activity is constrained by geometric distance. At each time step t, interactions of distance become active with probability τ. As for the local links whose activity rate $\tau = 1$, they stay active during the whole period to make every node reachable. All local connections and active shortcuts form the instantaneous network G_t. From the link's aspect, the dynamic correlation of link l during the observation time window T is defined as

$$\Gamma_l = \frac{1}{T-1} \sum_{t=1}^{T-1} l(t) \cdot l(t+1), \tag{3}$$

where $l(t) = 1$ if the link l is active at time t and $l(t) = 0$ otherwise. As each link intermittently switches between the states of "on" and "off", Γ_l quantitatively measures the ability of the link to persist its current state. Averaged over all shortcuts, $\Gamma = \langle \Gamma_l \rangle$ reflects the global persistence of the interaction dynamics.

Obviously, the basic properties of our model are determined by the common influence of Eqs. (1) and (2). In the case of $C = 0$, $\tau \to 1$ for any connection so that our model degrades to the static Kleinberg model with $\Gamma = 1$. Figure 1 vividly reflects the general persistence of the network for different C and α. For $\alpha > 2d$ ($d = 2$ in this work), most of the shortcuts are with small lengths [13] whose activity is scarcely influenced by spatial constraint, resulting in a highly clustered interaction pattern regardless of C. For $0 \leqslant \alpha \leqslant 2d$, there are shortcuts

of both short and long range, diverging in their ability to become active. When geometric constraint is in the reasonable scope, typically $C < 2$, the global persistence Γ is determined by the number of long-range shortcuts, which increases with descending α. With the increase of C, the spatial constraint on link dynamics becomes stronger and interactions are therefore poorly clustered in time, resulting in vigorously fluctuating topologies. When C grows to infinity, the network loses all potential long-range connections, degenerating to a stationary regular lattice.

III. OPTIMAL STRUCTURE OF TIME-VARYING NETWORKS

We now study in detail the dependence on the coupling strength C of the average temporal shortest path length $\langle T \rangle$. The nodes are located on a two-dimensional lattice with periodic boundaries. Here we assume that each node has two neighbors of long distance, namely, $q = 2$ [37]. Results depicted in Fig. 2 clearly indicate three regimes. For $C = 0$, the temporal effect disappears and the network degrades to a static Kleinberg model. As small α favors the creation of more shortcuts with long length, it significantly reduces the topological diameter. Hence the optimal value occurs at $\alpha = 0$ to maximize the transport efficiency, in accordance with the condition reported in previous literature [9,13,14]. In the temporal case, however, there is a contradiction. More shortcuts of long range, which greatly shorten the global transport path in static networks, lead to poorly clustered topologies because of their lower activity potential. In the intermediate range of $0 < C \leqslant 2$, an optimal exponent is always observed at $\alpha \neq 0$, in sharp contrast to the static case. With gradually deepening spatial constraint on link activities, α_{opt} slightly shifts to a larger value at around 2, balancing the temporal and geometric effect. For $C \gg 2$, $\langle T \rangle$ decays monotonically with α, since the shortcuts of long range
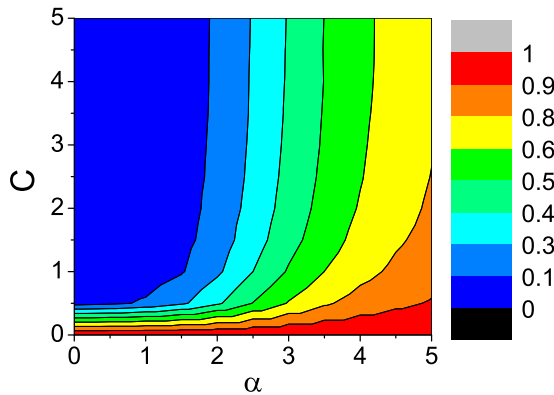

FIG. 1. Persistence of the interaction dynamics with different structural exponents α and coupling strengths C. For $C = 0$, the network degrades to a static model so that all shortcuts exist in the whole time period, resulting in the maximum persistence value of $\Gamma = 1$ regardless of α. With the growth of C, i.e., a stronger spatial constraint on link dynamics, the time persistence of long-range interactions is greatly reduced for the small structural exponent α. While in the large range of α, shortcuts of short range take charge, which are scarcely affected by spatial constraint.
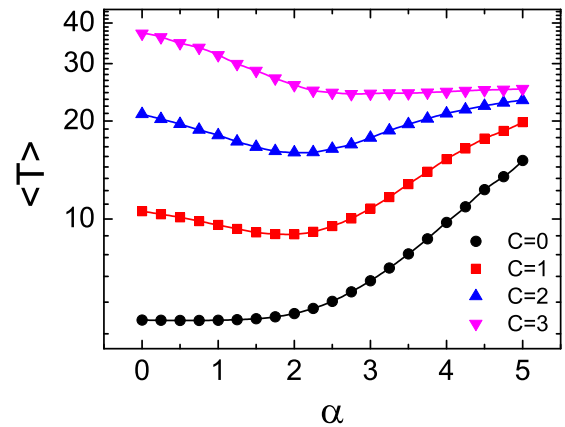

FIG. 2. Dependence on α of the average temporal shortest path length of the network for different values of C. The underlying substrate is a two-dimensional lattice with $L = 100$. The optimal structure for efficient navigation is found for three different regimes of C. For $C = 0$, the network degrades to a static Kleinberg model so that $\alpha_{\text{opt}} = 0$; for $0 < C \leqslant 2$, α_{opt} slightly grows around two; for $C \gg 2$, more long-range connections with poor activity will attenuate temporal diameter so that the optimal condition is $\alpha_{\text{opt}} \to \infty$.
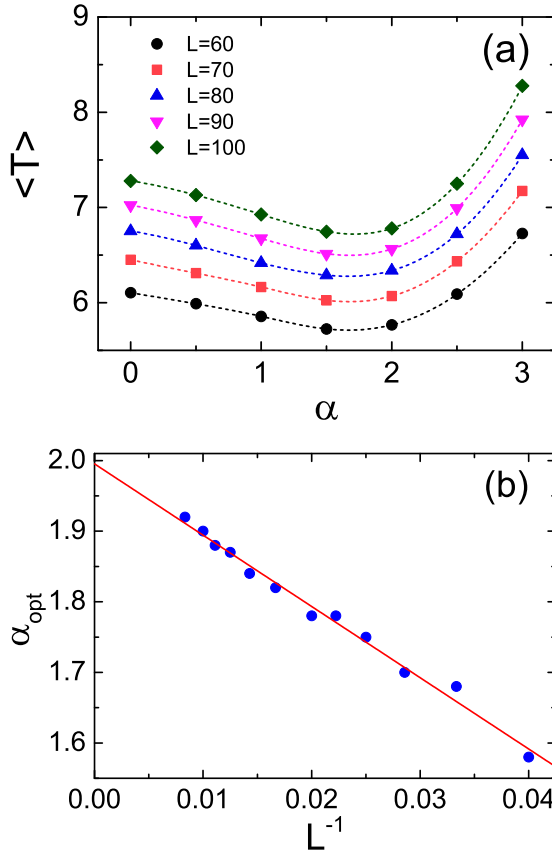
FIG. 3. (a) Average temporal shortest path length $\langle T \rangle$ versus α for different network sizes of $C = 0.5$. Nonmonotonical behavior of $\langle T \rangle$ has been observed with a minimum at $\alpha_{opt} \approx 1.9$ for $L = 100$. (b) Finite-size analysis presents $\alpha_{opt} = -10.09 \times L^{-1} + 1.99$ (fitted by red solid line), indicating that $\alpha_{opt} \to 2$ in the limit of $L \to \infty$. All the results are averaged with 100 realizations for $L = 60,70,80$, and 10 realizations for $L = 90,100$.
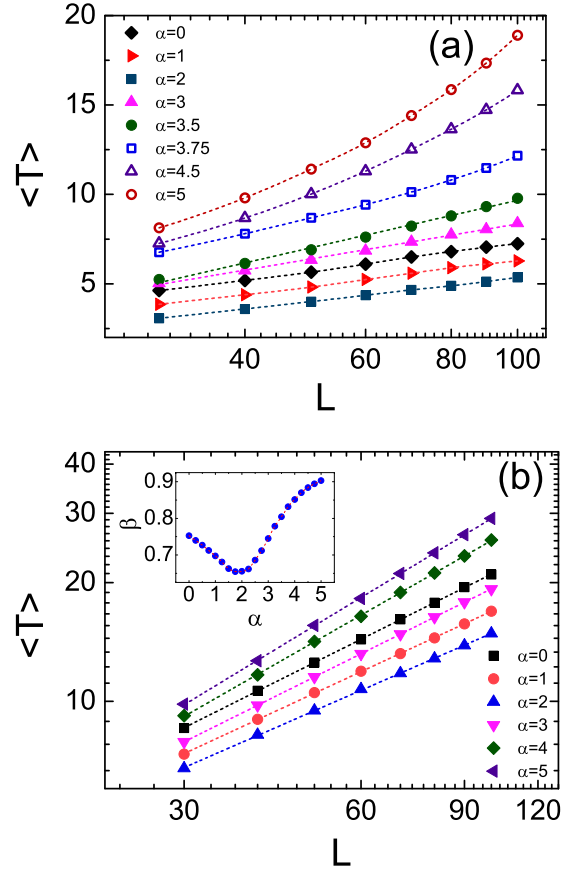

FIG. 4. Average temporal shortest path length $\langle T \rangle$ versus the linear size L of the network. (a) When $C = 0.5$, two distinctive behaviors are observed. For $0 \leqslant \alpha \leqslant 3.5$, $\langle T \rangle$ grows slowly as $\langle T \rangle \sim \log^{\gamma}(L)$, which is the signature of the small-world effect. For $\alpha > 3.5$, a power-law relation $\langle T \rangle \sim L^{\beta}$ emerges. (b) In the case of $C = 2$, however, only the power-law relation remains in the full range. As an indicator of the growth rate, the value of β falls at a minimum at $\alpha \approx 2$, as shown in the inset. Both plots have been vertically shifted for better visualization.

severely participate in this case. The minimum value of $\langle T \rangle$ is therefore obtained at $\alpha \to \infty$.

To quantitatively investigate the optimal structure for global transport, we further perform extensive simulations for different values of α and different system sizes. Here we present detailed results of $C = 0.5$ in Fig. 3(a). Intuitively, the average temporal shortest path length $\langle T \rangle$ behaves nonmonotonically with the structural exponent α. The minimum path length appears at $\alpha_{opt} \approx 2$ for large networks of size L, where the transport efficiency is best optimized. To get the precise α_{opt} of $L \to \infty$, we apply the finite-size scaling analysis. As shown in Fig. 3(b), the result of least linear fitting gives $\alpha_{opt} = -10.09 \times L^{-1} + 1.99$, which confirms the optimal exponent directly observed in Fig. 3(a).

We also show the way in which $\langle T \rangle$ scales with the system size L. For $C = 0.5$, the results in Fig. 4(a) clearly indicate two distinctive behaviors separated by a threshold $\alpha_c = 3.5$. For $0 \leqslant \alpha \leqslant \alpha_c$, a logarithmic relation, $\langle T \rangle \sim \log^{\gamma} L$, is observed, which is a signature of the small-world effect [1,38]. For those α tested out of this range, however, a power-law dependence of $\langle T \rangle \sim L^{\beta}$ takes over, indicating a large world. In the case of $C = 2$, however, all the $\langle T \rangle$ scale as $\langle T \rangle \sim L^{\beta}$, regardless of the value that α takes. And the minimal scaling exponent β

corresponds to the shortest $\langle T \rangle$, though the network cannot be a small world. As shown in the inset of Fig. 4(b), the minimum β is located at $\alpha \approx 2$, which indicates a relatively optimal structure.

To better reflect the influence of spatial constraint on long-range shortcuts, we perform similar analysis on other values of C in the range of $0 < C < 2$, where the small-world effect is available. As depicted in Fig. 5, the optimal structure exponent α_{opt} logarithmically increases, while the upper bound of the small-world region linearly decreases from 4 to 2, as shown in the inset of Fig. 5.

The above observations indicate the following conclusions. In time-varying systems with $0 < C < 2$, there exists an optimal spatial structure, resulting from the balance of geometric lengths and activity potential of shortcuts. In this effective range, the optimal exponent α_{opt} grows with gradually deepening constraints as $\alpha_{opt} \sim \log(C)$. Specifically, the optimal value for $C = 0.5$ is consist with the optimal condition $\alpha_{opt} = 2$ in static spatial networks navigated with local knowledge [2,3,7,8]. But once the coupling strength
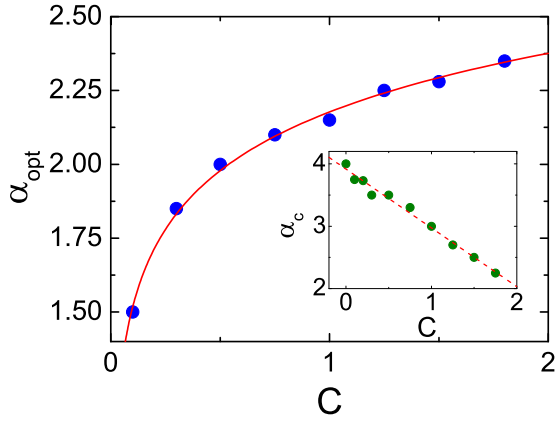
FIG. 5. Optimal structure exponent α_{opt} of different C. Intuitively, α_{opt} logarithmically increases with the deepening spatial constraint (red solid line) in the range of $0 < C < 2$. On the other hand, the separation threshold α_c reduces with C in a linear form, as shown in the inset.

exceeds the critical value of $C = 2$, the network is no longer efficient in information transport and the small-world region disappears.

IV. EMPIRICAL RESULTS OF AIRLINE NETWORKS

The airline network is a typical complex system exhibiting small-world features in which nodes are airports located in the plane with well-defined longitude and latitude. Two airports are connected once there is at least an air route, and this link is "on" if there is a running flight. The flight information is collected from official websites [39,40], and the geographical location of each airport is provided by the Open-Flights program [41]. Flights operate on a designed timetable, resulting in time-fluctuating interaction graphs of each day as illustrated in Fig. 6 [42].

The cumulated number of flights during a given period Δt (Δt is set to one week in this study due to the flight period) partially involves the information of how busy a certain line is. Flight intensity is closely related to the expected traffic on each air route. Due to the structural heterogeneity, the traffic w_{ij} over the air route depends on the degrees k_i, k_j of the airports located at both ends. As previously mentioned in [18], a power-law behavior of $w_{ij} \sim (k_i k_j)^\theta$ is observed in the world wide airport networks. Despite the divergence in airport capacity, the geographical distance of each air route, which is the proxy for transport cost, influences the flight intensity as well. Here we define the rescaled flight intensity $n_l = \frac{N_l}{k_i k_j}$, where l is the air route between airports i and j, and N_l is the number of cumulated flights during a week.

Intriguingly, results depicted in Figs. 7(a) and 7(b) clearly show a power-law dependence of the flight intensity on its geometric distance, i.e., $n_l \sim (r_l)^{-0.5}$. And the universal coupling exponents in both British and Austrian Airlines indicate that there is some intrinsic constraint restricting activity intensity in airline networks.

We also measured the probability density function (PDF) of the flight distances. For long-range flights, typically those with a distance larger than 10^3 km, the distribution decays
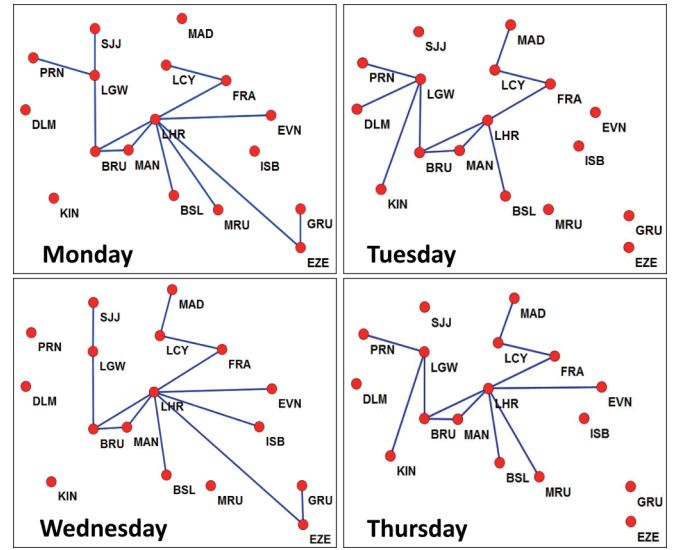

FIG. 6. An illustration of the temporal evolution of British Airways. For clarity, only a small part of the network is displayed. Nodes are arranged based on their relative geographical distances, and the label of each node is the airport's three-letter code. When there is a running flight between two airports, the link is "on" of that day. Otherwise, the link is hibernating and is not shown in the graph. Intuitively, the interaction structure varies day by day based on operation schedule and the air routes of long distance seem more volatile.
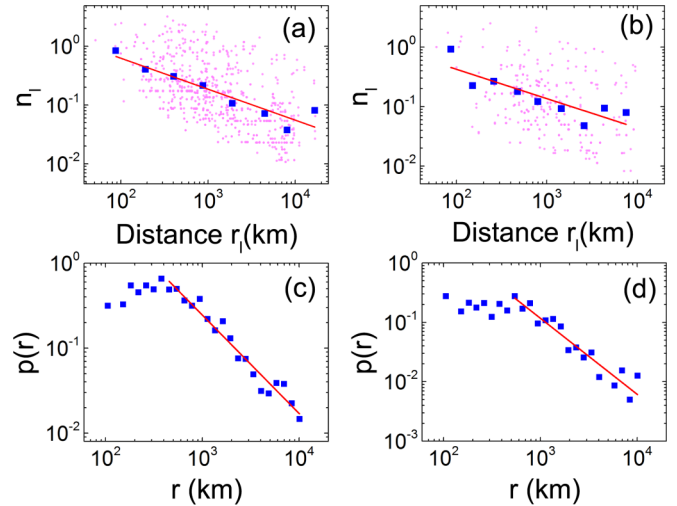

FIG. 7. Dependence of rescaled flight intensity on geometric distance for (a) British Airways and (b) Austrian Airlines. Logarithmically binned results (blue square) indicate a power-law dependence $n_l \sim (r_l)^{-C}$ in both companies. Least linear fitting derives a slope of -0.52 in British Airways and -0.49 in Austrian Airlines, respectively. The universal coupling exponents suggest some intrinsic constraint restricting activity intensity in airline networks. The distance distribution $p(r)$ of fights decays approximately as a power law $p(r) \sim r^{-\delta}$ for distance $> 10^3$ km with a structure exponent (c) $\delta \approx 1.15$ for British Airways and (d) $\delta \approx 1.2$ for Austrian Airlines.

approximately as a power law $p(r) \sim r^{-\delta}$ with an exponent $\delta \approx 1.15$ for British Airways and $\delta \approx 1.2$ for Austrian Airlines. In the d-dimensional lattice, the number of nodes that have the same distance r to a given node is proportional to r^{d-1}. Given the probability $P(r_{ij})$ for two nodes to have a long-range connection with length r, the PDF of the flight distances is

$$p(r) \sim r^{d-1} r^{-\alpha} = r^{d-\alpha-1}, \qquad (4)$$

which means $\delta = \alpha + 1 - d$. Hence the structural exponents of these two airline networks are $\alpha_{\text{British}} = \delta + 1 = 2.15$ and $\alpha_{\text{Austria}} = 2.2$, respectively, which is very close to the model prediction of $\alpha_{\text{opt}} = 2$ with the same coupling strength of $C = 0.5$. This consistence is not a coincidence. Deeply influenced by economic and social limitations, the design of air routes and corresponding running schedules reveals the optimized aspect of networks. After long-term self-organization, airline systems eventually evolve to be optimal. Similarly, the unique restriction between C and α indicates a general scheduling principle for other transport systems.

V. CONCLUSION

We propose a time-varying model to get insight about how the temporal aspect takes effect on the optimal structure for global transport. Here the geometric structure and interaction dynamics are entangled by associating power laws for both

(i) the probability distribution of long-range connections, $P_{ij} \sim r_{ij}^{-\alpha}$, and (ii) their corresponding activity potential, $\tau_{ij} \sim r_{ij}^{-C}$. For $C = 0$, our model degrades to the classical Kleinberg model with the optimal exponent $\alpha_{\text{opt}} = 0$ [9,13,14]. When the temporal dimension takes effect, namely, $C \neq 0$, the optimal transport occurs in a new structure. In the limit of large values of C, the spatial constraint is so strong that only short-range connections with significant activity potential contribute to improving the transport efficiency, and thus we obtained $\alpha_{\text{opt}} \to \infty$. For intermediate values $0 < C < 2$, the network behaves as a small world and the optimal structural exponent logarithmically grows with the coupling strength C. The difference between optimum conditions mainly results from the practical impact that long-range connections have on the transportation process. A similar work on Laplacian transport in small-world networks, in which the contribution of shortcuts is denoted by conductance, revealed the same fact [10]. With empirical validation in real air-transport systems, our observations suggest a design principle in temporal network optimization.

Notably, our model is not limited in geographic-based systems. As a measure of node similarity, the geometric distance also spans to social ones such as salary, research community, and friendship closeness. Therefore the idea of introducing the temporal effect in this framework offers a different view to explain the spatial scaling $p(r) \sim r^{-1}$ observed in many social networks [43–45].

[1] D. J. Watts and S. H. Strogatz, Nature (London) **393**, 440 (1998).
[2] J. M. Kleinberg, Nature (London) **406**, 845 (2000).
[3] J. M. Kleinberg, in *Proceedings of the Thirty-Second Annual ACM Symposium on Theory of Computing* (ACM, New York, 2000), p. 163.
[4] M. Boguñá, D. Krioukov, and K. C. Claffy, Nat. Phys. **5**, 74 (2008).
[5] L. Daqing, K. Kosmidis, A. Bunde, and S. Havlin, Nat. Phys. **7**, 481 (2011).
[6] M. R. Roberson and D. ben-Avraham, Phys. Rev. E **74**, 017101 (2006).
[7] S. Carmi, S. Carter, J. Sun, and D. ben-Avraham, Phys. Rev. Lett. **102**, 238702 (2009).
[8] C. Caretta Cartozo and P. De Los Rios, Phys. Rev. Lett. **102**, 238703 (2009).
[9] G. Li, S. D. S. Reis, A. A. Moreira, S. Havlin, H. E. Stanley, and J. S. Andrade, Jr., Phys. Rev. E **87**, 042810 (2013).
[10] C. L. N. Oliveira, P. A. Morais, A. A. Moreira, and J. S. Andrade, Jr., Phys. Rev. Lett. **112**, 148701 (2014).
[11] H. Yang, Y. Nie, A. Zeng, Y. Fan, Y. Hu, and Z. Di, Europhys. Lett. **89**, 58002 (2010).
[12] A. Zeng, D. Zhou, Y. Hu, Y. Fan, and Z. Di, Physica A (Amsterdam, Neth.) **390**, 3962 (2011).
[13] K. Kosmidis, S. Havlin, and A. Bunde, Europhys. Lett. **82**, 48005 (2008).
[14] C. F. Moukarzel and M. Argollode Menezes, Phys. Rev. E **65**, 056709 (2002).
[15] G. Li, S. D. S. Reis, A. A. Moreira, S. Havlin, H. E. Stanley, and J. S. Andrade, Jr., Phys. Rev. Lett. **104**, 018701 (2010).

[16] Y. Li, D. Zhou, Y. Hu, J. Zhang, and Z. Di, Europhys. Lett. **92**, 58002 (2010).
[17] W. Liu, A. Zeng, and Y. Zhou, Europhys. Lett. **98**, 28003 (2012).
[18] A. Barrat, M. Barthelemy, R. Pastor-Satorras, and A. Vespignani, Proc. Natl. Acad. Sci. USA **101**, 3747 (2004).
[19] R. Guimera, S. Mossa, A. Turtschi, and L. N. Amaral, Proc. Natl. Acad. Sci. USA **102**, 7794 (2005).
[20] A. Gautreau, A. Barrat, and M. Barthelemy, Proc. Natl. Acad. Sci. USA **106**, 8847 (2009).
[21] D.-D. Han, J.-H. Qian, and J.-G. Liu, Physica A (Amsterdam, Neth.) **388**, 71 (2009).
[22] J.-H. Qian, D.-D. Han, and Y.-G. Ma, Acta Phys. Sin. **60**, 098901 (2011).
[23] P. Holme, Phys. Rev. E **71**, 046119 (2005).
[24] S. A. Hill and D. Braha, Phys. Rev. E **82**, 046105 (2010).
[25] J. Tang, S. Scellato, M. Musolesi, C. Mascolo, and V. Latora, Phys. Rev. E **81**, 055101 (2010).
[26] R. K. Pan and J. Saramäki, Phys. Rev. E **84**, 016105 (2011).
[27] P. Holme and J. Saramäki, Phys. Rep. **519**, 97 (2012).
[28] H. Kim and R. Anderson, Phys. Rev. E **85**, 026107 (2012).
[29] S. Trajanovski, S. Scellato, and I. Leontiadis, Phys. Rev. E **85**, 066105 (2012).
[30] N. Perra, A. Baronchelli, D. Mocanu, B. Gonçalves, R. Pastor-Satorras, and A. Vespignani, Phys. Rev. Lett. **109**, 238701 (2012).
[31] A.-L. Barabási, Nature (London) **435**, 207 (2005).
[32] D.-D. Han, J.-G. Liu, and M. Yu-Gang, Chin. Phys. Lett. **25**, 765 (2008).

[33] N. Perra, B. Gonçalves, R. Pastor-Satorras, and A. Vespignani, Sci. Rep. **2**, 469 (2012).

[34] Q. Chen, J.-H. Qian, and D.-D. Han, Int. J. Mod. Phys. C **25**, 1440012 (2014).

[35] J.-H. Qian, Q. Chen, D.-D. Han, Y.-G. Ma, and W.-Q. Shen, Phys. Rev. E **89**, 062808 (2014).

[36] To bound τ in the interval $0 < \tau < 1$ for $r \in [2, r_{\max}]$, we impose a small disturbance and make a rescaling so that the activity potential can be accurately denoted as $\tau_{ij} = \frac{(r_{ij} + \delta)^{-C}}{2^{-C}}$, where $\delta \ll 1$.

[37] The parameter q does not make any effect on the relationship between T and L but only influences the average transport time.

[38] M. E. J. Newman and D. J. Watts, Phys. Rev. E **60**, 7332 (1999).

[39] Austrian Airlines, http://www.austrian.com.

[40] British Airways, http://www.britishairways.com.

[41] OpenFlights Project, http://openflights.org/data.html.

[42] All graphs are drawn in VisualNet, a visualization software developed under the JUNG framework by our own laboratory.

[43] D. Liben-Nowell, J. Novak, R. Kumar, P. Raghavan, and A. Tomkins, Proc. Natl. Acad. Sci. USA **102**, 11623 (2005).

[44] L. Adamic and E. Adar, Social Networks **27**, 187 (2005).

[45] R. Lambiotte, V. D. Blondel, C. de Kerchove, E. Huens, C. Prieur, Z. Smoreda, and P. Van Dooren, Physica A (Amsterdam, Neth.) **387**, 5317 (2008).